

Application of Hydroxyapatite Obtained by Different Techniques: Metabolism and Microarchitecture Characteristics (Review)

DOI: 10.17691/stm2024.16.6.06

Received April 17, 2024



V.A. Markelov, PhD Student, Institute of Biochemistry and Genetics¹; Junior Researcher, Laboratory of Cell Cultures, Institute of Fundamental Medicine²;

K.V. Danilko, PhD, Associate Professor, Department of Biology, Acting Head of Cell Culture Laboratory, Institute of Fundamental Medicine²;

V.A. Solntsev, Junior Researcher, Cell Culture Laboratory, Institute of Fundamental Medicine²;

S.V. Pyatnitskaya, PhD, Associate Professor, Department of Internal Diseases; Senior Researcher, Cell Culture Laboratory, Institute of Fundamental Medicine²;

A.R. Bilyalov, PhD, Associate Professor, Department of Traumatology and Orthopedics with a Course of the Institute of Continuing Professional Education²

¹Ufa Federal Research Center, Russian Academy of Sciences, 71 Oktyabr Avenue, Republic of Bashkortostan, Ufa, 450054, Russia;

²Bashkir State Medical University, 3 Lenin St., Republic of Bashkortostan, Ufa, 450008, Russia

The literature reports on microarchitecture and metabolism characteristics of synthetic hydroxyapatite obtained by different techniques were analyzed. The direct relation between hydroxyapatite production process and its microarchitecture was stated to exist. In turn, hydroxyapatite microarchitecture largely specifies its metabolism characteristics (a number of processes related to calcium and phosphorus metabolism). Therefore, with reference to the metabolism of synthetic hydroxyapatite with various microarchitectures, we analyzed the relationship of the material under study with the immune system cells.

Particular emphasis was given to the relationship of hydroxyapatite characteristics with a recipient's immune system due to the material microarchitecture. The review assessed the possible participation of cell mitochondria in synthetic hydroxyapatite metabolism. There were compared the findings of a recipient's immune system *in vivo* and *in vitro* depending on hydroxyapatite nanoscale morphology.

The review conclusions emphasized the necessity for further investigations of immunologically mediated metabolism of hydroxyapatite intended for bone implants, including the development of research methods *in vitro* for deeper understanding of the material properties. There was demonstrated the synthetic hydroxyapatite potential in treating bone defects and specified the significance of *in vivo* studies to develop bone surgery and reconstructive medicine.

Key words: hydroxyapatite; bone grafting; hydroxyapatite metabolism; microarchitecture.

How to cite: Markelov V.A., Danilko K.V., Solntsev V.A., Pyatnitskaya S.V., Bilyalov A.R. Application of hydroxyapatite obtained by different techniques: metabolism and microarchitecture characteristics (review). *Sovremennye tehnologii v medicine* 2024; 16(6): 60, <https://doi.org/10.17691/stm2024.16.6.06>

This is an open access article under the CC BY 4.0 license (<https://creativecommons.org/licenses/by/4.0/>).

Introduction

Current medical technologies dealing with bone tissue regeneration improvement are based on the extensive application of both hydroxyapatite-based grafts and implants. The variety of the materials used reflects a great number of pathological conditions of

bone tissue. According to the source, grafts are divided into autologous (autogenic), allogenic, and xenogeneic. In turn, the implants for bone regeneration can be conditionally divided by the material origin used for their production. The key value for bone implant production is synthetic hydroxyapatite made using chemical synthesis. However, there are many materials based on processed

Corresponding author: Vitaly A. Markelov, e-mail: vamarkelov@bashgmu.ru

hydroxyapatite of biogenic origin obtained using various processing techniques.

The use of autologous bone grafts is a recognized gold standard of bone grafting. In clinical practice autologous transplantation has already been usefully employed for a century [1, 2]. However, despite the fact that autologous material is standard, the number of studies aimed at searching for some alternative materials keeps growing. It is due to critical drawbacks of the methods used to obtain autologous material: firstly, limited volume of transplantation material [3, 4]; secondly, possible complications on a donor's site [5, 6]. A general list of complications includes infections, hematomas, chronic pain, fractures, as well as vessel and nerve damage [7]. The volume of the material taken out correlates with the complication risk [8] significantly limiting the use of autologous bone grafting. Therefore, it is extremely important to use alternative transplant materials, among them there are allogenic [9–11] and xenogeneic [10, 12]; that is why they under extensive study.

Allogenic material is functionally the most approximate one to autologous transplant material among those mentioned above. Its main advantage is relatively high availability [13]. Therefore, it has been widely used for long years in clinical practice to reconstruct extensive bone injuries. Like autogenous, allogeneic transplant material has a high degree of similarity to the native bone structure. It has similar mechanical properties, as well as osteoinductive and osteoconductive properties, and to some extent it is biocompatible. The specified properties are limited due to the necessity for the transplant material decellularization [11]. According to some authors, the main problem of the method is the absence of integrated protocols and a potential risk of transmitting infectious diseases [14].

The category of xenogeneic bone grafts has a number of similarities to allogenic materials. For instance, there are evidences confirming high osteoconductive properties of xenogeneic bovine bone material [15]. However, the independent use of xenogeneic graft, despite an uneventful postoperative period in certain cases [16], shows low quality of clinical results [17, 18]. The main negative results of xenotransplantation are fibrous graft encapsulation [19], vicious union, and pain syndrome [20]. Moreover, due to extremely high duration of xenograft integration (57 weeks) compared to an allograft (16 weeks), many experts cast doubt on the possibility of independent usage of xenogeneic grafts [17].

Thus, it is still urgent to solve the problem of standardization and high risk of transmitting infectious agents when transplanting allogenic [21, 22] or xenogeneic [23] bone materials. High risk of an increased immune response in allogenic and xenogeneic bone grafting is needed to be taken into consideration [24, 25]. The presented problems in using allogenic and xenogeneic grafts cause the necessity for developing safer, more available, and comparatively efficient alternative techniques.

Therefore, it is reasonable to use synthetic hydroxyapatite as a base for grafts, which enable them to take on the role of functional alternatives to bone grafts. It is proved by the experience of clinical use of hydroxyapatite [26–29]. Its popularity can be explained by the fact that hydroxyapatite is a native form of bone tissue calcium, it occupying 70–90% of its matrix volume. In bone tissue, hydroxyapatite is in the form of small-sized crystals and characterized by a stoichiometric formula: $\text{Ca}_{10}(\text{PO}_4)_6(\text{OH})_2$ [30]. Special attention is drawn by a composite form of using synthetic hydroxyapatite, since the native bone is also a composite structure [31, 32].

Hydroxyapatite was shown to contribute to bone tissue regeneration providing favorable osteoimmune microenvironment [33]. However, even if the materials most suitable for obtaining bone grafts are used, a preliminary detailed analysis of an immune response is required. Within the given context, a number of unique immunological parameters of hydroxyapatite-based materials can acquire great importance [34, 35]. Modern literature data [33, 36, 37] demonstrate an immunomodulating effect of hydroxyapatite-based materials. So, there was studied a macrophage-mediated regenerative effect of hydroxyapatite related to the graft material metabolism [33]. Such information enables to manipulate these parameters adjusting structural and textural material characteristics, as well as including various functional components. The relationship of synthetic hydroxyapatite nanostructural parameters and its immunomodulating properties is still an open issue [33]. There are left unclarified the hydroxyapatite metabolism parameters on a cell level; and the role of monocytes/macrophages in particular [33, 38].

Sourcing methodology

The literature for the present review was searched in MEDLINE (PubMed) and Google Scholar by key words and their combinations: hydroxyapatite bone grafts, hydroxyapatite nanoparticles, nanostructured hydroxyapatite, bone grafts for biomedical applications, hydroxyapatite synthesis for bone grafts, hydroxyapatite for biomedical applications, hydroxyapatite production for bone grafting, biogenic hydroxyapatite, dry method hydroxyapatite production, dry method of hydroxyapatite production, chemical method of hydroxyapatite production, osteoclast response to synthetic hydroxyapatite, response to synthetic hydroxyapatite, properties of nanostructured hydroxyapatite, osteogenic potential of hydroxyapatite, osteoconductive potential of hydroxyapatite.

Available scientific data was gained till November 28, 2023. The articles were selected by two coauthors, independently from one another using manual search. All differences were smoothed by means of discussions by an authoring team, as well as by consulting the third expert. A total of 133 scientific articles were selected.



Figure 1. Algorithm of solid-phase method of hydroxyapatite production:

1 — source of calcium raw material (calcium hydroxide); 2 — source of phosphates (ammonium hydrophosphate); 3 — optional introduction of salts; 4 — prepared calcium phosphate powder; 5 — intensive mechanical grinding (vibrating ball mill); 6 — high-temperature treatment of the mixture; 7 — transferring material in the form of primary raw material. The illustration was created using the online tool BioRender (<https://www.biorender.com/>)

Synthetic hydroxyapatite production processes and synthetic hydroxyapatite nanostructure characteristics

There are two main categories of preparation techniques: solid-phase methods and those using solvents [39].

Solid-phase methods are characterized by using a mechanical action and relatively high temperatures (Figure 1).

The methods require no solvents [40, 41]. A solid-phase technology has low sensitivity to production conditions [42, 43] and generates a product with high crystallization [39, 44]. However, such hydroxyapatite often includes intermediate phases [45] and exhibits low biomimetic properties [46]. On the other hand, such material production is easily scaled using the optimal temperature of 1050°C. So, high temperatures for hydroxyapatite production slightly decrease its porosity [45], it being the significant restriction of its usage as a material for bone grafting.

Chemical deposition methods are characterized by using solvents — the sources of calcium and phosphates [39] — in the presence of additives [47–50] in acid or basic media (Figure 2). The range of production conditions of these methods is extremely diverse: there is a great variability of pH values (3–12) [51, 52] and temperatures (25–90°C) [39, 53].

Precipitation enables to obtain hydroxyapatite particles with native morphology (needle-like) [54] and makes it possible to manipulate it [40]. Precipitation provides the preparation of the material with desired ion-

substitution by magnesium [47], strontium, lithium [55], manganese [48], aluminium [49], zinc [55, 56], selenium [50], and other metals [57, 58].

Chemical deposition is used to obtain a composite material [59] forming the coating for polymer [60–62], metal [63, 64], and combined scaffolds [65, 66]. Through this process, there can be obtained composite porous micelles [67], nanoparticles [68], nanotubes [69], and nanorods [70]. Hydroxyapatite obtained through chemical deposition has low crystallinity [40]. Despite chemical deposition requires no high temperatures, the method needs the strict control of synthesis conditions. On the one hand, it decreases hydroxyapatite production scaling by the method, although, on the other hand, it enables the fine adjustment of the hydroxyapatite morphology and nanoparticle size [53]. It is likely to be an important advantage when using the method in research practice.

An electrochemical method is based on aqueous solutions [71]. The technique enables to form a uniform coating at moderate temperatures, providing strong integration of hydroxyapatite into porous agents [71, 72]. A striking example is the method of impulse electrodeposition, which decreases the release of gaseous hydrogen, improving hydroxyapatite integration [71]. Similarly to chemical deposition, electrodeposition is used to produce composite structures of hydroxyapatite with the most diverse morphology and composition [73]. Such structures can include different alloys [74–76], including aluminium ones [77], and polymer bases [78]. The abovementioned electric deposition also has morphological variety: hydroxyapatite nanotubes [79],

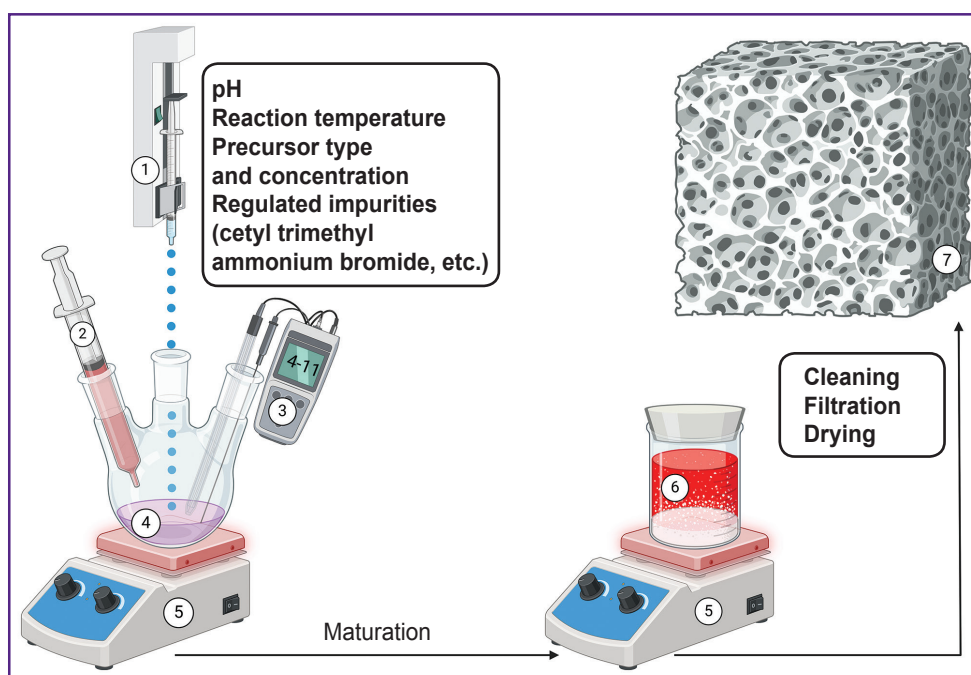


Figure 2. Algorithm for obtaining hydroxyapatite by chemical deposition:

1 — a syringe pump with Ca^{2+} reagent (calcium nitrate $\text{Ca}(\text{NO}_3)_2$); 2 — pH controller (ammonium solution); 3 — pH meter; 4 — phosphate anions (diammonium phosphate $(\text{NH}_4)_2\text{HPO}_4$); 5 — stirring and temperature control; 6 — precipitation of hydroxyapatite particles; 7 — transfer material in the form of primary raw material. The illustration was created using the BioRender online tool (<https://www.biorender.com/>)

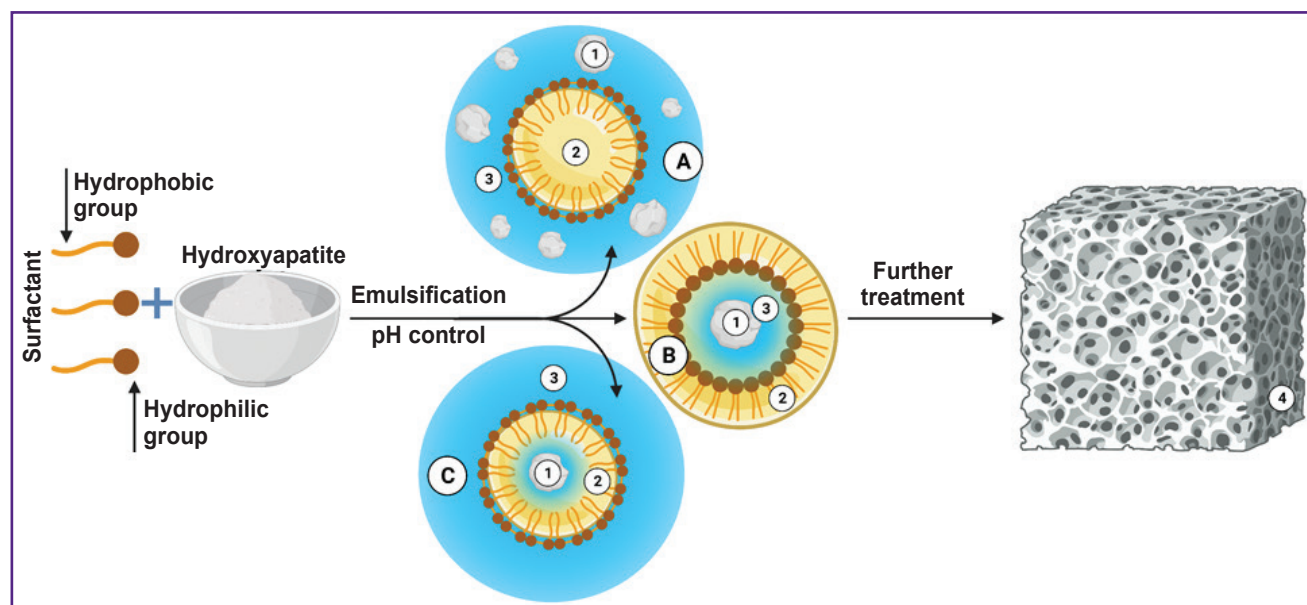


Figure 3. Algorithm for hydroxyapatite production using emulsion method:

1 — hydroxyapatite particles; 2 — oil phase; 3 — aqueous phase; 4 — implantation material; A — oil encapsulated in an aqueous phase containing particles; B — oil encapsulates an aqueous phase with a hydroxyapatite particle; C — emulsion system, where an aqueous phase contains the oil with an encapsulated aqueous medium containing hydroxyapatite particle. The illustration was created using the BioRender online tool (<https://www.biorender.com/>)

nanoparticles [80], and other disperse hydroxyapatite forms [81, 82, 57].

Emulsion method belonging to category 2 methods

is one of the most effective for obtaining nanostructural hydroxyapatite powder (Figure 3). Powder particles form in a disperse medium of two immiscible solvents

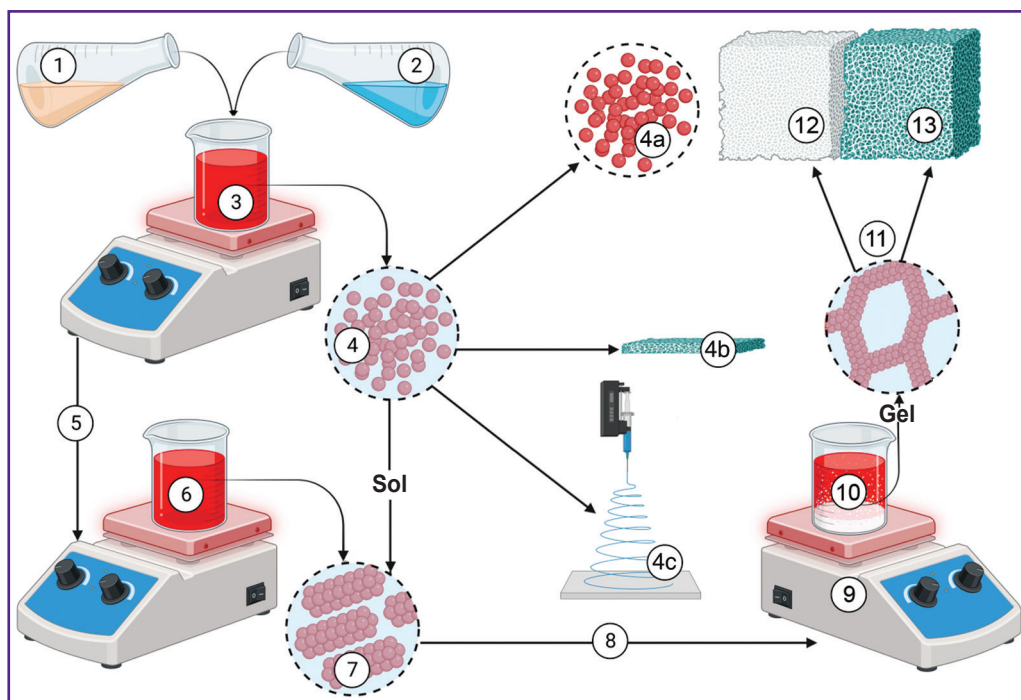


Figure 4. Sol-gel method operation scheme:

1 — phosphate-containing reagent (phosphorus pentoxide); 2 — calcium-containing reagent (calcium nitrate); 3 — solvent (water or ethanol), control of sol formation reaction; 4 — sol condition of the reaction mixture (4a — deposition with the material formed as powder; 4b — formation of coatings; 4c — formation of ceramic fibers); 5 — the reaction mixture transfer from sol to gel; 6 — control of coagulation reaction parameters; 7 — coagulation; 8 — direct transfer into gel-formation condition; 9 — control over gel-formation reaction conditions; 10 — gel; 11 — evaporation and extraction by a dissolvent; 12 — aerogel formation; 13 — dense ceramics. The illustration was created using the BioRender online tool (<https://www.biorender.com/>)

stabilized by surface-active agents (SAA). The way the emulsion is produced is determined by SAA nature and concentration [83]. An emulsion provides a favorable medium to regulate particle growth. In turn, hydrophobic SAA are easily removed by ignition [84, 85].

The emulsion method advantage is the strict control of morphological parameters of nanoparticles, and due to this the technique is often used to obtain porous materials. The sources of calcium and phosphate can be calcium nitrate and phosphoric acid. As SAA, there can be used dioctyl sodium sulfosuccinate, dodecyl phosphate, polyoxyethylene, non-polyphenol ether, polyoxyethylene ether, cetyl trimethyl ammonium bromide, and sodium dodecyl sulfate. In addition to SAA characteristics, end parameters of hydroxyapatite can be determined by temperature, water and organic phase relationship, pH and precursors concentration [39].

Sol-gel method is a relatively popular method to obtain hydroxyapatite (Figure 4). As precursors, there can be used calcium chloride and various organic phosphites [86]. It is convenient for obtaining film coatings [87, 88] and aerogel structures [39]. The technique presupposes precursors hydrolysis with the formation of micelles associated with templates in aqueous or organic media. It provides high chemical

homogeneity of hydroxyapatite [89], appropriate stoichiometry, and minimal size clustering. There were additionally indicated high rate of surface-specific area and available mesoporous volume of hydroxyapatite obtained by the method [90]. *In vitro* studies confirm good biodegradation characteristics of the material obtained by this method [40]. However, it has a limited scaling potential due to low availability of precursors. Moreover, insufficient manufacturing control can promote the formation of secondary phases in the form of CaO , $\text{Ca}_2\text{P}_2\text{O}_7$, $\text{Ca}_3(\text{PO}_4)_2$, and CaCO_3 [39].

Each of the methods presented has its advantages; therefore, the most logical step towards improving synthetic hydroxyapatite quality can be the combination of the above-described methods of its production. So, an emulsion method product, for example, undergoes high-temperature treatment [84], which is often a final stage of combined technologies, and enhances the material crystallinity [85]. There are two main variants of high-temperature treatment as separate methods. They are pyrolytic spraying and a sputter coating technique. The first one consists of spraying a solution of calcium and phosphorus salts in a high-temperature furnace followed by water evaporation and the formation of hydroxyapatite crystals. The second technique presupposes high-

temperature coating of the target by hydroxyapatite. In both cases the morphology and size of the particles can be regulated, since the parameters directly depend on the characteristics of sprayed and evaporated drops [40].

Biogenic sources of hydroxyapatite

Let us consider the most common techniques used to produce hydroxyapatite from biogenic sources, their popular raw material is biological waste: great cattle bones [91, 92], egg shell [93, 94], sea organisms [95–98], and plants. The latter can be used to extract hydroxyapatite [99] or as a solvent [100, 101]. In addition, they are used as calcium [102] and phosphate [103, 104] sources. Literature reports demonstrate the applicability of nanostructural hydroxyapatite of plant origin [105] and mycogenous hydroxyapatite [106].

The key requirement for this raw material type is the possibility to remove organic residues, it being achieved

through heat treatment [93], subcritical water treatment [107, 108], alkaline thermal hydrolysis [108], and fermentation techniques [109].

Natural hydroxyapatite has different substitution degrees of such elements as Na⁺, Zn²⁺, Mg²⁺, K⁺, Si²⁺, Ba²⁺, F⁻, and CO₃²⁻ [110]. It explains the multiple roles of native hydroxyapatite of bone tissue. There was described high biomimeticity of the obtained hydroxyapatite and the mineral phase of human bone [93]. It was confirmed by the data indicating the similarity of leading morphological and micro-architectural parameters of hydroxyapatite treated at high temperatures [111]. So, the specific surface and morphology of synthesized hydroxyapatite particles are in the range of the values characteristic for native bone tissue [112–115]. It should be noted that biogenic hydroxyapatite can serve as raw material source for many production methods of synthetic hydroxyapatite (see the Table [92, 93, 95, 96, 98, 115–123]).

Application of different biogenic raw material types to obtain hydroxyapatite

Source of raw materials	Method of extraction	Description of an end product (hydroxyapatite)	<i>In vitro</i> and <i>in vivo</i> study findings	References
Animal bone waste	Ignition	Hexagonal nanoparticles, 300–500 nm in size	Good viability and proliferation of cells	[92, 115]
	Treatment using a ball mill	Nanoparticles, under 500 nm in size	Osteogenic differentiation of dental stem cells	[116]
<i>M. furnieri</i> waste	NaOH and H ₂ O ₂ treatment, t=800°C	Particles with pores ~8 μm in size	Tissue growing in a graft	[95, 117]
<i>H. molitrix</i> bone waste	NaOH and acetone treatment	Powder, average crystallite size ~58.3 nm	MG63 cell viability is 91%	[118]
	Ignition, t=900°C	Powder, average crystallite size ~64.3 nm	MG63 cell viability is 86%	
<i>Tilapia</i> bone waste	Ignition, t=600–800°C	Porous grains with high Mg ²⁺ substitution degree	High biocompatibility degree	[114]
<i>E. chlorostigma</i> bone waste	Alkaline hydrolysis and ignition, t=600°C	Nanoparticles, 29.5 and 82.12 nm in size, respectively	High biocompatibility degree of L929 cells. High remineralization potential	[119]
<i>L. catla</i> and <i>N. japonicus</i> scales	Ignition, t=800°C and treatment using a ball mill	Porous nanoparticles, 30–60 nm in size, and 10-nm crystallites	In combination with polycaprolactone, there was proliferation and perfect adhesion indices	[98]
<i>L. lentjan</i> scale	Hydrothermal treatment, t=280°C	Rods 50–100 nm long, 8–12 nm in diameter, and spheroids 15–50 nm in diameter	Biocompatibility and high osteogenic potential of human mesenchymal stem cells	[120]
Plancton	Leaching of solid particles	Porous nanohydroxyapatite	Adhesion, proliferation, and viability	[121]
<i>A. glabrata</i> shells	Ignition, t=900°C and deposition	Nanoscale rods 13.3–15.2 nm	Inhibits development of pathogenic bacteria and fungi	[96]
<i>Sepia</i> cuttlefish skeleton	Heat treatment NH ₄ H ₂ PO ₄ , t=200°C	Biomimetic microspheres 1–2 μm	MG63 proliferation. High alkaline phosphatase activity and osteocalcin expression	[122]
<i>A. fulica</i> shells	Sintering in the presence of (NH ₄) ₂ HPO ₄ In succession: t=150°C (night), 80°C (up to complete drying), 750°C (1 h)	Nanoparticles, 87.7–88.9 nm in size	Antibacterial activity	[123]

Source of raw materials	Method of extraction	Description of an end product (hydroxyapatite)	<i>In vitro</i> and <i>in vivo</i> study findings	References
Egg shell	H ₃ PO ₄ heat treatment In succession: t=80°C (night), 150°C (24 h), 80°C (24 h)	Particles 21.0–40.8 nm containing Mg and Sr	High cell adhesion of MG63 cells	[93]

The presence of a great variety of alternative methods for obtaining synthetic hydroxyapatite using the most diverse precursors provides great opportunities to produce bone grafts with various nanostructural parameters. It is due to the described above dependence of hydroxyapatite nanoarchitecture on its production methods. The nanostructure variety is an important condition for choosing the research and therapeutic strategies for bone graft application.

Metabolism and interaction characteristics with the recipient's immune system

Most grafts used for bone tissue regeneration are temporary structures, which provide structural support, contribute to bone repair, and direct bone growth. Semi-synthetic and synthetic materials are available and can be modified (for instance, there can be confirmed the positive dynamics of new bone formation based on hydroxyapatite scaffold [124].

Among the most common synthetic bone expletive substances, there is a group of calcium-phosphate ceramics, including hydroxyapatite, β-tricalcium phosphate, and α-tricalcium phosphate, calcium sulphate, as well as bioactive glass and polymers [125]. Hydroxyapatite has a number of characteristics compared to other synthetic bone substitutes. Compared to β-tricalcium phosphate, carbonate-substituted hydroxyapatite [126, 127] exhibits increased solubility under the conditions imitating lacunas of Howship (resorption fossae) [128]. The latter structure is the result of osteoclastic activity and plays an important role in bone remodeling [129]. β-tricalcium phosphate resorption is maximum in physiologically normal conditions [128]. Even higher resorption in physiological conditions was found for α-tricalcium phosphate [130]. In addition, it should be noted that hydroxyapatite substituted by magnesium exhibits lower resorption in bone defects compared to hemihydrate of calcium sulphate [131]. In its turn, calcium sulphate demonstrates incomplete osteogenic response compared to β-tricalcium phosphate/apatite [132, 133].

When comparing hydroxyapatite and bioactive glass, there is a striking osteoinductive response of the latter [125]. It is due to an amorphous layer formed on the glass surface providing the conditions for the concentration of structural proteins and growth factors

[134]. A comparative analysis of hydroxyapatite, bioactive glass, and composites containing both materials showed the increase in osteoconductive potential when hydroxyapatite was added [135]. Apart from that, the grafts based on composite materials made of hydroxyapatite and bioactive glass exhibit higher mechanical stability after implantation compared to a pure bioglass material [135, 136].

The comparison of hydroxyapatite grafting and bioactive glass grafting demonstrates the greater area of neoformed bone and the greater number of TRAP-positive (TRAP — tartrate-resistant acid phosphatase) cells when using hydroxyapatite [137]. TRAP-positive cells are mostly presented by osteoclasts and macrophages [138, 139].

The distinctive feature of hydroxyapatite behavior under bone remodeling against the background described in the works [137, 139] can be a particular relation of the material with osteoclastic activity.

As for polymer synthetic bone substitutes, there is a similar tendency for osteogenic potential increase under conditions of including hydroxyapatite into their composition [140]. When there is used the polyurethane composite with 40% hydroxyapatite added, the capacity for *in vitro* biomineralization and osteogenic differentiation increases. Similarly, *in vivo* studies indicated the considerable volume of vascularized bone tissue [141]. There is the same tendency when hydroxyapatite is included in polyethylene glycol diacrylate composition: the improved mechanical properties and biocompatibility are exhibited [142, 143].

The data presented suggest the interaction of hydroxyapatite with TRAP-positive cells [137, 144–146], in particular, with osteoclasts and their immune precursors [138, 139]. The relationship between hydroxyapatite and a marked acute immune response in recipients is confirmed by aseptic destruction and bone tissue osteolysis in response to the material implantation. The response directly depends on the presence of hydroxyapatite particles, under 53 μm in size, decreasing the viability of osteoblasts and osteoclasts [147]. The mentioned response to small-sized hydroxyapatite is characteristic for different cells, including tumor ones; hydroxyapatite particles inhibit their proliferation due to protein synthesis inhibition, blocking the accessibility of ribosomes for mRNA [148]. In addition, it should be noted that nanosized hydroxyapatite initiates selective

apoptosis [36] and blocks melanoma growth [149]. It is foremost related to the disturbed cell homeostasis of calcium and the activation of endogenous mitochondrial stimuli of apoptosis [81] that seems intriguingly in the scope of hypothesis of mitochondrial mineralization of bone tissue [38]. Moreover, hydroxyapatite enables to initiate monocytes flattening and the differentiation of macrophages into osteoclast-associated phenotype. Hydroxyapatite effect stimulates the expression of a nuclear factor kappa B ligand and the podosome belt formation in monocytes/macrophages, the activity of osteoclasts being modulated [150, 151].

It should be noted that the hydroxyapatite treated using the method of solution and deposition compared to untreated hydroxyapatite promotes TRAP-positive staining area growth. The index is associated with the osteoclastic activity. The differences under observation are explained by the presence of the nanoscale hydroxyapatite in untreated material, whereas untreated material exhibits coarse-grain structure [152]. It is in good agreement with the fact that plate-like nanostructure of hydroxyapatite is associated with active cell proliferation at early co-incubation stages. On the contrary, for hydroxyapatite with needle-like nanostructure, high cell proliferation is found only at late experiment stages. Plate-like hydroxyapatite microstructure is also related to the greater number of flattened macrophages [153].

There was procured valid evidence in favor of the effect hydroxyapatite particle morphology has on cytokine synthesis by mouse dendritic cells. The highest IL-1 β (interleukin 1 β) secretion was found in the response to needle-like hydroxyapatite. In contrast, there was found no capability to enhance IL-1 β synthesis for spherical particles, ~100 μ m in size. It was expected that in intraperitoneal administration, needle-like hydroxyapatite particles cause the stronger inflammatory response compared to their spherical analogs. In mouse peritoneal exudate cells stimulated by needle-like particles, ~5 μ m in size, higher TNF- α (tumor necrosis factor alpha) levels were found in response to re-stimulation. All exudate samples, other than those stimulated by spherical particles, ~100 μ m in size, showed decreased IL-10 production. In combination with the dynamics of infiltration by mast cells and macrophages, it indicates the less inflammatory response to large spherical particles compared to needle-like ones [37]. Moreover, the material particle morphology plays a key role in forming osteoconductive properties owing to the material resorption rate regulated by TRAP-positive osteoclast-like cells [154].

Comparatively, later studies also have confirmed the particular importance of the nanoscale morphology of the hydroxyapatite-based graft material. For instance, hydroxyapatite with grooved structure compared to the control hydroxyapatite promotes better macrophage attachment and decreases the production of anti-inflammatory cytokines of TNF- α , IL-1 β , and IL-6. The phenomenon is due to the decreased accumulation of

reactive oxygen species (ROS) owing to the modulation of mitochondrial functions. However, no effect on the character and dynamics of macrophage polarization was revealed [155], although the later studies have reported on such a possibility [35]. On the other hand, in case of nanostructural hydroxyapatite action on macrophages, there is an increase in the synthesis of TNF- α , IL-6, adenosine triphosphate, nicotinamide adenine dinucleotide, and ROS [156]. At the same time, CD8-positive T-cells demonstrate increased expression of IFN- γ and CD107 α [157]. In contrast, micro-grooved structure decreases IL-6 expression owing to inhibiting miR-214, and thus contributing to the survival of mesenchymal bone marrow stem cells [155]. The rod-like hydroxyapatite ability to have an effect on mitochondrial functionality is proved by its antitumor action mechanism. For example, in nano-rod hydroxyapatite internalization, mitochondrial ROS and cathepsin B are released [157]. The hydroxyapatite with the mentioned morphology demonstrates marked immunomodulating [33, 36] and proapoptotic [36] properties.

Next literature example [148] demonstrates the difference in the properties of hydroxyapatite with different morphology under *in vivo* and *in vitro* conditions. *In vivo* studies showed a comparable osteogenic potential for both nanostructural and submicron hydroxyapatite. Moreover, nanostructural hydroxyapatite exhibits greater osteogenic potential. Concurrently, the authors emphasized the relationship of osteogenesis and osteoclastogenesis. However, in *in vitro* experiments nanostructural hydroxyapatite has an inhibiting effect concerning the early differentiation and survival of osteoclasts. It decreases the expression of specific markers of osteoclastogenesis, as well as TRAP activity, including ROS-generating activity. Therefore, it is noteworthy that there are reports on ribosomal and mitochondrial mechanisms of inhibiting cell activity by hydroxyapatite [36, 148]. Meanwhile, submicron hydroxyapatite in *in vitro* experiments is able to have a stimulating effect in relation to osteoclast differentiation and activity [133].

To conclude, it is important to note Ca²⁺ content analysis indicates decreased osteoclastogenesis at early incubation stages of RAW 264.7 cells with nanostructural hydroxyapatite. However, on day 14 the researchers observed the gradual increase and sustaining this osteoclastogenesis characteristic. However, in a similar experiment for submicron hydroxyapatite, on day 14 there was the registered steep downfall of this osteoclastogenesis characteristic that can be due to osteoclastic apoptosis.

There are some studies, which have shown the activating properties of nanostructural hydroxyapatite regarding osteoclasts [152]. The observed contradiction can be due to the differences in infiltration parameters of immune cells in *in vivo* and *in vitro* experiments (e.g., the infiltration dynamics of macrophages and mast cells in nanostructural hydroxyapatite grafting

[37]). It is not unlikely that the observed phenomenon has ROS-dependent mitochondrial origin and is associated with apoptosis. The implication is that the nature of the phenomenon under study is complex since the effect of differences in the infiltration stability parameters of immune cells is not exclusive of ROS-dependent mitochondrial mechanism of osteoclastic apoptosis. Thus, the further advance in the phenomenon comprehension requires integrated studies including the assessment of such molecular mechanisms as ROS-dependent mitochondrial apoptotic cascades.

Conclusion

According to the data presented, synthetic hydroxyapatite as a bone graft material exhibits high osteogenic potential and is capable of stimulating osteoclastic activity. The comparative analysis showed the use of hydroxyapatite as a component of composite materials to enhance mechanical stability and osteoconductive properties of grafts.

There is the hypothesis describing the bone tissue mineralization as the energy-dependent movement of calcium cations and phosphate anions of blood serum into osteoblastic mitochondria followed by the deposition of amorphous microbatches of calcium phosphate. The hypothesis is successfully consistent with the literature data confirming a significant role of mitochondria in the metabolism of both synthetic and native hydroxyapatite. On the other hand, synthetic hydroxyapatite and native hydroxyapatite have a positive effect on mitochondrial ROS-dependent functions. However, the character of such an effect directly depends on hydroxyapatite microarchitecture. The represented facts enable to distinguish the main direction of future research. For instance, it is necessary to reveal certain metabolic mechanisms of synthetic hydroxyapatite of bone grafts by determining the role of mitochondrial apparatus of cells.

The represented literature data make rather complete picture of differences between *in vivo* and *in vitro* study findings of synthetic hydroxyapatite with different nanoscale morphology. Primarily, they enable to conclude that the adequate assessment of hydroxyapatite as an implantation material with nanoscale morphology, as for now, is possible only if there is relatively constant and long-time infiltration of immune cells. These conditions to the full extent can be achieved in *in vivo* studies. However, we are aware of the need for checking the declaration by further target research.

In addition, among the key characteristics of hydroxyapatite as a material for bone grafts, there can be specified its specific character of interacting with monocytes/monophages, osteoclasts, and T-cells of the recipient's body. Moreover, this characteristic can be directly regulated by the nanoscale morphology of the material providing the preservation of its macroscopic

structure. In this context, particular interest can be provoked by the ability of nanostructural hydroxyapatite to have an effect on ribosomes and mitochondria of many cells including tumor cells. Combined with satisfactory mechanical properties, high scaling potential, and the production process unification, the material can be used to treat major bone defects. It is worth noting separately the defects resulting from tumor removal, that are due to an antitumor effect of nanostructural hydroxyapatite. However, the issue also has to be elaborated using target studies.

Authors contribution. V.A. Markelov, A.R. Bilyalov — study concept development; V.A. Markelov, V.A. Solntsev — literature search and collection; V.A. Markelov, K.V. Danilko, S.V. Pyatnitskaya — article text writing; V.A. Markelov, K.V. Danilko — methodology; V.A. Markelov, V.A. Solntsev — imaging; K.V. Danilko, S.V. Pyatnitskaya, A.R. Bilyalov — formal analysis; V.A. Markelov, K.V. Danilko, S.V. Pyatnitskaya, A.R. Bilyalov, V.A. Solntsev — scientific editing; A.R. Bilyalov, K.V. Danilko, S.V. Pyatnitskaya — general management. All authors read the text and agreed to publish the present manuscript version.

Study funding. The study was supported by Russian Science Foundation (project No.23-15-20042).

Conflict of interest. The authors declare no conflict of interest.

References

- Schmidt A.H. Autologous bone graft: is it still the gold standard? *Injury* 2021; 52(Suppl 2): S18–S22, <https://doi.org/10.1016/j.injury.2021.01.043>.
- Dissaux C., Ruffenach L., Bruant-Rodier C., George D., Bodin F., Rémond Y. Cleft alveolar bone graft materials: literature review. *Cleft Palate Craniofac J* 2022; 59(3): 336–346, <https://doi.org/10.1177/10556656211007692>.
- Kobbe P., Laubach M., Hutmacher D.W., Alabdulrahman H., Sellei R.M., Hildebrand F. Convergence of scaffold-guided bone regeneration and RIA bone grafting for the treatment of a critical-sized bone defect of the femoral shaft. *Eur J Med Res* 2020; 25(1): 70, <https://doi.org/10.1186/s40001-020-00471-w>.
- Ehredt D.J. Jr, Rogers B., Takhar J., Payton P., Siesel K. Percutaneous harvest of calcaneal bone autograft: quantification of volume and definition of anatomical safe zone. *J Foot Ankle Surg* 2022; 61(1): 27–31, <https://doi.org/10.1053/j.jfas.2021.06.001>.
- van de Wall B.J.M., Beeres F.J.P., Rompen I.F., Link B.C., Babst R., Schoeneberg C., Michelitsch C., Nebelung S., Pape H.C., Gueorguiev B., Knoke M. RIA versus iliac crest bone graft harvesting: a meta-analysis and systematic review. *Injury* 2022; 53(2): 286–293, <https://doi.org/10.1016/j.injury.2021.10.002>.
- Laubach M., Weimer L.P., Bläsius F.M., Hildebrand F., Kobbe P., Hutmacher D.W. Complications associated using the reamer-irrigator-aspirator (RIA) system: a systematic review and meta-analysis. *Arch*

- Orthop Trauma Surg* 2023; 143(7): 3823–3843, <https://doi.org/10.1007/s00402-022-04621-z>.
7. Dimitriou R., Mataliotakis G.I., Angoules A.G., Kanakaris N.K., Giannoudis P.V. Complications following autologous bone graft harvesting from the iliac crest and using the RIA: a systematic review. *Injury* 2011; 42(Suppl 2): S3–S15, <https://doi.org/10.1016/j.injury.2011.06.015>.
 8. Suda A.J., Schamberger C.T., Viergutz T. Donor site complications following anterior iliac crest bone graft for treatment of distal radius fractures. *Arch Orthop Trauma Surg* 2019; 139(3): 423–428, <https://doi.org/10.1007/s00402-018-3098-3>.
 9. Li G., Li P., Chen Q., Thu H.E., Hussain Z. Current updates on bone grafting biomaterials and recombinant human growth factors implanted biotherapy for spinal fusion: a review of human clinical studies. *Curr Drug Deliv* 2019; 16(2): 94–110, <https://doi.org/10.2174/1567201815666181024142354>.
 10. Smeets R., Matthies L., Windisch P., Gosau M., Jung R., Brodala N., Stefanini M., Kleinheinz J., Payer M., Henningsen A., Al-Nawas B., Knipfer C. Horizontal augmentation techniques in the mandible: a systematic review. *Int J Implant Dent* 2022; 8(1): 23, <https://doi.org/10.1186/s40729-022-00421-7>.
 11. Sharifi M., Kheradmandi R., Salehi M., Alizadeh M., Ten Hagen T.L.M., Falahati M. Criteria, challenges, and opportunities for acellularized allogeneic/xenogeneic bone grafts in bone repairing. *ACS Biomater Sci Eng* 2022; 8(8): 3199–3219, <https://doi.org/10.1021/acsbiomaterials.2c00194>.
 12. Salem D., Alshihri A., Arguello E., Jung R.E., Mohamed H.A., Friedland B. Volumetric analysis of allogeneic and xenogenic bone substitutes used in maxillary sinus augmentations utilizing cone beam CT: a prospective randomized pilot study. *Int J Oral Maxillofac Implants* 2019; 34(4): 920–926, <https://doi.org/10.11607/jomi.7318>.
 13. Lomas R., Chandrasekar A., Board T.N. Bone allograft in the U.K.: perceptions and realities. *Hip Int* 2013; 23(5): 427–433, <https://doi.org/10.5301/hipint.5000018>.
 14. Scheuffler K.M., Diesing D. Use of bone graft replacement in spinal fusions. *Orthopade* 2015; 44(2): 146–153, <https://doi.org/10.1007/s00132-014-3069-5>.
 15. Tawil G., Barbeck M., Unger R., Tawil P., Witte F. Sinus floor elevation using the lateral approach and window repositioning and a xenogeneic bone substitute as a grafting material: a histologic, histomorphometric, and radiographic analysis. *Int J Oral Maxillofac Implants* 2018; 33(5): 1089–1096, <https://doi.org/10.11607/jomi.6226>.
 16. Ding Y., Wang L., Su K., Gao J., Li X., Cheng G. Horizontal bone augmentation and simultaneous implant placement using xenogeneic bone rings technique: a retrospective clinical study. *Sci Rep* 2021; 11(1): 4947, <https://doi.org/10.1038/s41598-021-84401-8>.
 17. Shibuya N., Holloway B.K., Jupiter D.C. A comparative study of incorporation rates between non-xenograft and bovine-based structural bone graft in foot and ankle surgery. *J Foot Ankle Surg* 2014; 53(2): 164–167, <https://doi.org/10.1053/j.jfas.2013.10.013>.
 18. Shibuya N., Jupiter D.C. Bone graft substitute: allograft and xenograft. *Clin Podiatr Med Surg* 2015; 32(1): 21–34, <https://doi.org/10.1016/j.cpm.2014.09.011>.
 19. Schwarz F., Ferrari D., Balic E., Buser D., Becker J., Sager M. Lateral ridge augmentation using equine- and bovine-derived cancellous bone blocks: a feasibility study in dogs. *Clin Oral Implants Res* 2010; 21(9): 904–912, <https://doi.org/10.1111/j.1600-0501.2010.01951.x>.
 20. Ledford C.K., Nunley J.A. 2nd, Viens N.A., Lark R.K. Bovine xenograft failures in pediatric foot reconstructive surgery. *J Pediatr Orthop* 2013; 33(4): 458–463, <https://doi.org/10.1097/BPO.0b013e318287010d>.
 21. Ruffilli A., Barile F., Fiore M., Manzetti M., Viroli G., Mazzotti A., Govoni M., De Franceschi L., Dallari D., Faldini C. Allogeneic bone grafts and postoperative surgical site infection: are positive intraoperative swab cultures predictive for a higher infectious risk? *Cell Tissue Bank* 2023; 24(3): 627–637, <https://doi.org/10.1007/s10561-022-10061-1>.
 22. Singh S., Verma A., Jain A., Goyal T., Kandwal P., Arora S.S. Infection and utilization rates of bone allografts in a hospital-based musculoskeletal tissue bank in north India. *J Clin Orthop Trauma* 2021; 23: 101635, <https://doi.org/10.1016/j.jcot.2021.101635>.
 23. Van Der Merwe W., Lind M., Faunø P., Van Egmond K., Zaffagnini S., Marcacci M., Cugat R., Verdonk R., Ibañez E., Guillen P., Marcheggiani Muccioli G.M. Xenograft for anterior cruciate ligament reconstruction was associated with high graft processing infection. *J Exp Orthop* 2020; 7(1): 79, <https://doi.org/10.1186/s40634-020-00292-0>.
 24. Graham S.M., Leonidou A., Aslam-Pervez N., Hamza A., Panteliadis P., Heliotis M., Mantalaris A., Tsiridis E. Biological therapy of bone defects: the immunology of bone allo-transplantation. *Expert Opin Biol Ther* 2010; 10(6): 885–901, <https://doi.org/10.1517/14712598.2010.481669>.
 25. Hinsenkamp M., Muylle L., Eastlund T., Fehily D., Noël L., Strong D.M. Adverse reactions and events related to musculoskeletal allografts: reviewed by the World Health Organisation Project NOTIFY. *Int Orthop* 2012; 36(3): 633–641, <https://doi.org/10.1007/s00264-011-1391-7>.
 26. Pang Y.X., Liu X.W., Huang J.L., Zuo H.J., Xu X., Pei X.F. Identification of the strain which highly produces protease and β -D-glucosidase isolated from shuidouchi produced in sichuan and evaluating its ability of producing protease. *Sichuan Da Xue Xue Bao Yi Xue Ban* 2019; 50(5): 714–719.
 27. George S.M., Nayak C., Singh I., Balani K. Multifunctional hydroxyapatite composites for orthopedic applications: a review. *ACS Biomater Sci Eng* 2022; 8(8): 3162–3186, <https://doi.org/10.1021/acsbiomaterials.2c00140>.
 28. Zaed I., Cardia A., Stefani R. From reparative surgery to regenerative surgery: state of the art of porous hydroxyapatite in cranioplasty. *Int J Mol Sci* 2022; 23(10): 5434, <https://doi.org/10.3390/ijms23105434>.
 29. Sobczyk-Guzenda A., Boniecka P., Laska-Lesniewicz A., Makowka M., Szymanowski H. Micro- and nanoparticulate hydroxyapatite powders as fillers in polyacrylate bone cement—a comparative study. *Materials (Basel)* 2020; 13(12): 2736, <https://doi.org/10.3390/ma13122736>.
 30. Giordana A., Malandrino M., Zambon A., Lusvardi G., Operti L., Cerrato G. Biostimulants derived from organic urban wastes and biomasses: an innovative approach. *Front Chem* 2023; 11: 969865, <https://doi.org/10.3389/fchem.2023.969865>.

31. Gao C., Peng S., Feng P., Shuai C. Bone biomaterials and interactions with stem cells. *Bone Res* 2017; 5: 17059, <https://doi.org/10.1038/boneres.2017.59>.
32. Zimmermann E.A., Ritchie R.O. Bone as a structural material. *Adv Healthc Mater* 2015; 4(9): 1287–1304, <https://doi.org/10.1002/adhm.201500070>.
33. Shang L., Shao J., Ge S. Immunomodulatory properties: the accelerant of hydroxyapatite-based materials for bone regeneration. *Tissue Eng Part C Methods* 2022; 28(8): 377–392, <https://doi.org/10.1089/ten.TEC.2022.00111112>.
34. Mahon O.R., Browe D.C., Gonzalez-Fernandez T., Pitacco P., Whelan I.T., Von Euw S., Hobbs C., Nicolosi V., Cunningham K.T., Mills K.H.G., Kelly D.J., Dunne A. Nanoparticle mediated M2 macrophage polarization enhances bone formation and MSC osteogenesis in an IL-10 dependent manner. *Biomaterials* 2020; 239: 119833, <https://doi.org/10.1016/j.biomaterials.2020.119833>.
35. Wang R., Hua Y., Wu H., Wang J., Xiao Y.C., Chen X., Ao Q., Zeng Q., Zhu X., Zhang X. Hydroxyapatite nanoparticles promote TLR4 agonist-mediated anti-tumor immunity through synergically enhanced macrophage polarization. *Acta Biomater* 2023; 164: 626–640, <https://doi.org/10.1016/j.actbio.2023.04.027>.
36. Zhang K., Zhou Y., Xiao C., Zhao W., Wu H., Tang J., Li Z., Yu S., Li X., Min L., Yu Z., Wang G., Wang L., Zhang K., Yang X., Zhu X., Tu C., Zhang X. Application of hydroxyapatite nanoparticles in tumor-associated bone segmental defect. *Sci Adv* 2019; 5(8): eaax6946, <https://doi.org/10.1126/sciadv.aax6946>.
37. Lebre F., Sridharan R., Sawkins M.J., Kelly D.J., O'Brien F.J., Lavelle E.C. The shape and size of hydroxyapatite particles dictate inflammatory responses following implantation. *Sci Rep* 2017; 7(1): 2922, <https://doi.org/10.1038/s41598-017-03086-0>.
38. Indurkar A., Choudhary R., Rubenis K., Locs J. Role of carboxylic organic molecules in interfibrillar collagen mineralization. *Front Bioeng Biotechnol* 2023; 11: 1150037, <https://doi.org/10.3389/fbioe.2023.1150037>.
39. Kien P.T., Phu H.D., Linh N.V.V., Quyen T.N., Hoa N.T. recent trends in hydroxyapatite (HA) synthesis and the synthesis report of nanostructure HA by hydrothermal reaction. *Adv Exp Med Biol* 2018; 1077: 343–354, https://doi.org/10.1007/978-981-13-0947-2_18.
40. Sadiq T.O., Sudin I., Idris J., Fadil N.A. Synthesis techniques of bioceramic hydroxyapatite for biomedical applications. *Journal of Biomimetics, Biomaterials and Biomedical Engineering* 2023; 59: 59–80, <https://doi.org/10.4028/p-yqw75e>.
41. Clabel H.J.L., Awan I.T., Pinto A.H., Nogueira I.C., Bezzon V.D.N., Leite E.R., Balogh D., Mastelaro V., Ferreira S., Marega E. Insights on the mechanism of solid state reaction between TiO₂ and BaCO₃ to produce BaTiO₃ powders: the role of calcination, milling, and mixing solvent. *Ceramics International* 2020; 46(3): 2987–3001, <https://doi.org/10.1016/j.ceramint.2019.09.296>.
42. Szczeńs A., Holysz L., Chibowski E. Synthesis of hydroxyapatite for biomedical applications. *Adv Colloid Interface Sci* 2017; 249: 321–330, <https://doi.org/10.1016/j.cis.2017.04.007>.
43. Chesley M., Kennard R., Roozbahani S., Kim S.M., Kuk K., Mason M. One-step hydrothermal synthesis with in situ milling of biologically relevant hydroxyapatite. *Mater Sci Eng C Mater Biol Appl* 2020; 113: 110962, <https://doi.org/10.1016/j.msec.2020.110962>.
44. Sathiyavimal S., Vasantharaj S., LewisOscar F., Pugazhendhi A., Subashkumar R. Biosynthesis and characterization of hydroxyapatite and its composite (hydroxyapatite-gelatin-chitosan-fibrin-bone ash) for bone tissue engineering applications. *Int J Biol Macromol* 2019; 129: 844–852, <https://doi.org/10.1016/j.ijbiomac.2019.02.058>.
45. Fihri A., Len C., Varma R.S., Solhy A. Hydroxyapatite: a review of syntheses, structure and applications in heterogeneous catalysis. *Coordination Chemistry Reviews* 2017; 347: 48–76, <https://doi.org/10.1016/j.ccr.2017.06.009>.
46. Qi M.L., He K., Huang Z.N., Shahbazian-Yassar R., Xiao G.Y., Lu Y.P., Shokuhfar T. Hydroxyapatite fibers: a review of synthesis methods. *JOM* 2017; 69(8): 1354–1360, <https://doi.org/10.1007/s11837-017-2427-2>.
47. Andrés N.C., D'Elia N.L., Ruso J.M., Campelo A.E., Massheimer V.L., Messina P.V. Manipulation of Mg²⁺-Ca²⁺ switch on the development of bone mimetic hydroxyapatite. *ACS Appl Mater Interfaces* 2017; 9(18): 15698–15710, <https://doi.org/10.1021/acsami.7b02241>.
48. Lala S., Ghosh M., Das P.K., Kar T., Pradhan S.K. Mechanical preparation of nanocrystalline biocompatible single-phase Mn-doped A-type carbonated hydroxyapatite (A-cHAp): effect of Mn doping on microstructure. *Dalton Trans* 2015; 44(46): 20087–20097, <https://doi.org/10.1039/c5dt03398e>.
49. Wang M., Wang L., Shi C., Sun T., Zeng Y., Zhu Y. The crystal structure and chemical state of aluminum-doped hydroxyapatite by experimental and first principles calculation studies. *Phys Chem Chem Phys* 2016; 18(31): 21789–21796, <https://doi.org/10.1039/c6cp03230c>.
50. Kolmas J., Kuras M., Oledzka E., Sobczak M. A solid-state NMR study of selenium substitution into nanocrystalline hydroxyapatite. *Int J Mol Sci* 2015; 16(5): 11452–11464, <https://doi.org/10.3390/ijms160511452>.
51. Lin D.J., Lin H.L., Haung S.M., Liu S.M., Chen W.C. Effect of pH on the in vitro biocompatibility of surfactant-assisted synthesis and hydrothermal precipitation of rod-shaped nano-hydroxyapatite. *Polymers (Basel)* 2021; 13(17): 2994, <https://doi.org/10.3390/polym13172994>.
52. Le H.R., Chen K.Y., Wang C.A. Effect of pH and temperature on the morphology and phases of co-precipitated hydroxyapatite. *Journal of Sol-Gel Science and Technology* 2011; 61(3): 592–599, <https://doi.org/10.1007/s10971-011-2665-7>.
53. Lee I.H., Lee J.A., Lee J.H., Heo Y.W., Kim J.J. Effects of pH and reaction temperature on hydroxyapatite powders synthesized by precipitation. *Journal of the Korean Ceramic Society* 2019; 57(1): 56–64, <https://doi.org/10.1007/s43207-019-00004-0>.
54. Wijesinghe W.P., Mantilaka M.M., Premalal E.V., Herath H.M., Mahalingam S., Edirisinghe M., Rajapakse R.P., Rajapakse R.M. Facile synthesis of both needle-like and spherical hydroxyapatite nanoparticles: effect of synthetic temperature and calcination on morphology, crystallite size and crystallinity. *Mater Sci Eng C Mater Biol Appl* 2014; 42: 83–90, <https://doi.org/10.1016/j.msec.2014.05.032>.
55. Boyd A.R., Rutledge L., Randolph L.D., Meenan B.J.

- Strontium-substituted hydroxyapatite coatings deposited via a co-deposition sputter technique. *Mater Sci Eng C Mater Biol Appl* 2015; 46: 290–300, <https://doi.org/10.1016/j.msec.2014.10.046>.
56. Robinson L., Salma-Ancane K., Stipniec L., Meenan B.J., Boyd A.R. The deposition of strontium and zinc Co-substituted hydroxyapatite coatings. *J Mater Sci Mater Med* 2017; 28(3): 51, <https://doi.org/10.1007/s10856-017-5846-2>.
57. Gu M., Li W., Jiang L., Li X. Recent progress of rare earth doped hydroxyapatite nanoparticles: luminescence properties, synthesis and biomedical applications. *Acta Biomater* 2022; 148: 22–43, <https://doi.org/10.1016/j.actbio.2022.06.006>.
58. Lakrat M., Jodati H., Mejdoubi E.M., Evis Z. Synthesis and characterization of pure and Mg, Cu, Ag, and Sr doped calcium-deficient hydroxyapatite from brushite as precursor using the dissolution-precipitation method. *Powder Technology* 2023; 413: 118026, <https://doi.org/10.1016/j.powtec.2022.118026>.
59. Shah R.K., Fahmi M.N., Mat A.H., Zainal A.A. The synthesis of hydroxyapatite through the precipitation method. *Med J Malaysia* 2004; 59(Suppl B): 75–76.
60. Chen W., Nichols L., Brinkley F., Bohna K., Tian W., Priddy M.W., Priddy L.B. Alkali treatment facilitates functional nano-hydroxyapatite coating of 3D printed polylactic acid scaffolds. *Mater Sci Eng C Mater Biol Appl* 2021; 120: 111686, <https://doi.org/10.1016/j.msec.2020.111686>.
61. Enami H., Nakahara I., Ando W., Uemura K., Hamada H., Takao M., Sugano N. Osteocompatibility of Si₃N₄-coated carbon fiber-reinforced polyetheretherketone (CFRP) and hydroxyapatite-coated CFRP with antibiotics and antithrombotic drugs. *J Artif Organs* 2023; 26(2): 144–150, <https://doi.org/10.1007/s10047-022-01340-5>.
62. Laschke M.W., Strohe A., Menger M.D., Alini M., Eglin D. In vitro and in vivo evaluation of a novel nanosize hydroxyapatite particles/poly(ester-urethane) composite scaffold for bone tissue engineering. *Acta Biomater* 2010; 6(6): 2020–2027, <https://doi.org/10.1016/j.actbio.2009.12.004>.
63. Chen J., Yang Y., Etim I.P., Tan L., Yang K., Misra R.D.K., Wang J., Su X. Recent advances on development of hydroxyapatite coating on biodegradable magnesium alloys: a review. *Materials (Basel)* 2021; 14(19): 5550, <https://doi.org/10.3390/ma14195550>.
64. Kalpana M., Nagalakshmi R. Nano hydroxyapatite for biomedical applications derived from chemical and natural sources by simple precipitation method. *Appl Biochem Biotechnol* 2023; 195(6): 3994–4010, <https://doi.org/10.1007/s12010-022-03968-8>.
65. Kuśmierczyk F., Fiolek A., Łukaszczyk A., Kopia A., Sitarz M., Zimowski S., Cieniek Ł., Moskalewicz T. Microstructure and selected properties of advanced biomedical n-HA/ZnS/Sulfonated PEEK coatings fabricated on zirconium alloy by duplex treatment. *Int J Mol Sci* 2022; 23(6): 3244, <https://doi.org/10.3390/ijms23063244>.
66. Hu H., Lin C., Leng Y. An investigation of HAP/organic polymer composite coatings prepared by electrochemical co-deposition technique. *Sheng Wu Yi Xue Gong Cheng Xue Za Zhi* 2003; 20(1): 4–7.
67. Zhang Y., Dong K., Wang F., Wang H., Wang J., Jiang Z., Diao S. Three dimensional macroporous hydroxyapatite/chitosan foam-supported polymer micelles for enhanced oral delivery of poorly soluble drugs. *Colloids Surf B Biointerfaces* 2018; 170: 497–504, <https://doi.org/10.1016/j.colsurfb.2018.06.053>.
68. Sivasankari S., Kalaivizhi R., Gowriboy N., Ganesh M.R., Shazia Anjum M. Hydroxyapatite integrated with cellulose acetate/polyetherimide composite membrane for biomedical applications. *Polymer Composites* 2021; 42(10): 5512–5526, <https://doi.org/10.1002/pc.26242>.
69. Akiyama N., Patel K.D., Jang E.J., Shannon M.R., Patel R., Patel M., Perriman A.W. Tubular nanomaterials for bone tissue engineering. *J Mater Chem B* 2023; 11(27): 6225–6248, <https://doi.org/10.1039/d3tb00905j>.
70. Adamu D.B., Zereffa E.A., Segne T.A., Razali M.H., Lemu B.R. Synthesis and characterization of bismuth-doped hydroxyapatite nanorods for fluoride removal. *Environmental Advances* 2023; 12: 100360, <https://doi.org/10.1016/j.envadv.2023.100360>.
71. Asri R.I., Harun W.S., Hassan M.A., Ghani S.A., Buyong Z. A review of hydroxyapatite-based coating techniques: sol-gel and electrochemical depositions on biocompatible metals. *J Mech Behav Biomed Mater* 2016; 57: 95–108, <https://doi.org/10.1016/j.jmbbm.2015.11.031>.
72. Kuo M.C., Yen S.K. The process of electrochemical deposited hydroxyapatite coatings on biomedical titanium at room temperature. *Materials Science and Engineering: C* 2002; 20(1–2): 153–160, [https://doi.org/10.1016/s0928-4931\(02\)00026-7](https://doi.org/10.1016/s0928-4931(02)00026-7).
73. Kumar S., Gupta R.K., Archana K., Kumari R. Development of ternary hydroxyapatite-Al₂O₃-TiO₂ nanocomposite coating on Mg alloy by electrophoretic deposition method. *Journal of Materials Engineering and Performance* 2023; 33(10): 5075–84, <https://doi.org/10.1007/s11665-023-08290-w>.
74. Baheti W., Lv S., Mila, Ma L., Amantai D., Sun H., He H. Graphene/hydroxyapatite coating deposit on titanium alloys for implant application. *J Appl Biomater Funct Mater* 2023; 21: 22808000221148104, <https://doi.org/10.1177/22808000221148104>.
75. Quraishi M.A., Chauhan D.S. Recent trends in the development of corrosion inhibitors. In: Kamachi Mudali U., Subba Rao T., Ningshen S., Pillai R.G., George R.P., Sridhar T.M. (eds). *A treatise on corrosion science, engineering and technology*. Indian Institute of Metals series. Springer, Singapore; 2002, https://doi.org/10.1007/978-981-16-9302-1_40.
76. Li G., Song Y., Chen X., Xu W., Tong G., Zhang L., Li J., Zhu X. Preparation, corrosion behavior and biocompatibility of MgFe-layered double hydroxides and calcium hydroxyapatite composite films on 316L stainless steel. *Materials Today Communications* 2023; 34: 105195, <https://doi.org/10.1016/j.mtcomm.2022.105195>.
77. Sundaramali G., Aiyasamy J.P., Karthikeyan S., Kandavel T.K., Arulmurugan B., Rajkumar S., Sharma S., Li C., Dwivedi S., Kumar A., Singh R., Eldin S. Experimental investigations of electrodeposited Zn–Ni, Zn–Co, and Ni–Cr–Co-based novel coatings on AA7075 substrate to ameliorate the mechanical, abrasion, morphological, and corrosion properties for automotive applications. *Reviews on Advanced Materials Science* 2023; 62(1), <https://doi.org/10.1515/rams-2022-0324>.

78. Al-Noaman A., Rawlinson S.C.F. Polyether ether ketone coated with nanohydroxyapatite/graphene oxide composite promotes bioactivity and antibacterial activity at the surface of the material. *Eur J Oral Sci* 2023; 131(5–6): e12946, <https://doi.org/10.1111/eos.12946>.
79. Gao Q., Zhang L., Chen Y., Nie H., Zhang B., Li H. Interfacial design and construction of carbon fiber composites by strongly bound hydroxyapatite nanobelt-carbon nanotubes for biological applications. *ACS Appl Bio Mater* 2023; 6(2): 874–882, <https://doi.org/10.1021/acsbm.2c01028>.
80. Park S.J., Jang J.M. Electrodeposition of hydroxyapatite nanoparticles onto ultra-fine TiO₂ nanotube layer by electrochemical reaction in mixed electrolyte. *J Nanosci Nanotechnol* 2011; 11(8): 7167–7171, <https://doi.org/10.1166/jnn.2011.4865>.
81. Zhang Q., Qiang L., Liu Y., Fan M., Si X., Zheng P. Biomaterial-assisted tumor therapy: a brief review of hydroxyapatite nanoparticles and its composites used in bone tumors therapy. *Front Bioeng Biotechnol* 2023; 11: 1167474, <https://doi.org/10.3389/fbioe.2023.1167474>.
82. Kargozar S., Mollazadeh S., Kermani F., Webster T.J., Nazamezhad S., Hamzehlou S., Baino F. Hydroxyapatite nanoparticles for improved cancer theranostics. *J Funct Biomater* 2022; 13(3): 100, <https://doi.org/10.3390/jfb13030100>.
83. Gómora-Figueroa A.P., Camacho-Velázquez R.G., Guadarrama-Cetina J., Guerrero-Sarabia T.I. Oil emulsions in naturally fractured Porous Media. *Petroleum* 2019; 5(3): 215–226, <https://doi.org/10.1016/j.petlm.2018.12.004>.
84. Liang Q., Liu X., Zeng G., Liu Z., Tang L., Shao B., Zeng Z., Zhangb W., Liua Y., Chenga M., Tanga W., Gongd S. Surfactant-assisted synthesis of photocatalysts: mechanism, synthesis, recent advances and environmental application. *Chemical Engineering Journal* 2019; 372: 429–451, <https://doi.org/10.1016/j.cej.2019.04.168>.
85. Sadat-Shojai M., Khorasani M.T., Dinpanah-Khoshdargi E., Jamshidi A. Synthesis methods for nanosized hydroxyapatite with diverse structures. *Acta Biomater* 2013; 9(8): 7591–7621, <https://doi.org/10.1016/j.actbio.2013.04.012>.
86. Ioițescu A., Vlase G., Vlase T., Ilia G., Doca N. Synthesis and characterization of hydroxyapatite obtained from different organic precursors by sol-gel method. *Journal of Thermal Analysis and Calorimetry* 2009; 96(3): 937–942, <https://doi.org/10.1007/s10973-009-0044-1>.
87. Yun Y.H., Lee J.K. Sol-gel coating of hydroxyapatite on zirconia substrate. *J Nanosci Nanotechnol* 2021; 21(8): 4169–4173, <https://doi.org/10.1166/jnn.2021.19375>.
88. Jaafar A., Hecker C., Árki P., Joseph Y. Sol-gel derived hydroxyapatite coatings for titanium implants: a review. *Bioengineering (Basel)* 2020; 7(4): 127, <https://doi.org/10.3390/bioengineering7040127>.
89. Ishikawa K., Garskaite E., Kareiva A. Sol-gel synthesis of calcium phosphate-based biomaterials — a review of environmentally benign, simple, and effective synthesis routes. *Journal of Sol-Gel Science and Technology* 2020; 94(3): 551–572, <https://doi.org/10.1007/s10971-020-05245-8>.
90. Molino G., Palmieri M.C., Montalbano G., Fiorilli S., Vitale-Brovarone C. Biomimetic and mesoporous nano-hydroxyapatite for bone tissue application: a short review. *Biomed Mater* 2020; 15(2): 022001, <https://doi.org/10.1088/1748-605X/ab5f1a>.
91. Hernández-Barreto D.F., Hernández-Cocoletzi H., Moreno-Piraján J.C. Biogenic hydroxyapatite obtained from bone wastes using CO₂-assisted pyrolysis and its interaction with glyphosate: a computational and experimental study. *ACS Omega* 2022; 7(27): 23265–23275, <https://doi.org/10.1021/acsomega.2c01379>.
92. Amna T. Valorization of bone waste of Saudi Arabia by synthesizing hydroxyapatite. *Appl Biochem Biotechnol* 2018; 186(3): 779–788, <https://doi.org/10.1007/s12010-018-2768-5>.
93. Wu S.C., Hsu H.C., Wang H.F., Liou S.P., Ho W.F. Synthesis and characterization of nano-hydroxyapatite obtained from eggshell via the hydrothermal process and the precipitation method. *Molecules* 2023; 28(13): 4926, <https://doi.org/10.3390/molecules28134926>.
94. Patel D.K., Jin B., Dutta S.D., Lim K.T. Osteogenic potential of human mesenchymal stem cells on eggshells-derived hydroxyapatite nanoparticles for tissue engineering. *J Biomed Mater Res B Appl Biomater* 2020; 108(5): 1953–1960, <https://doi.org/10.1002/jbm.b.34536>.
95. Prado J.P.D.S., Yamamura H., Magri A.M.P., Ruiz P.L.M., Prado J.L.D.S., Rennó A.C.M., Ribeiro D.A., Granito R.N. In vitro and in vivo biological performance of hydroxyapatite from fish waste. *J Mater Sci Mater Med* 2021; 32(9): 109, <https://doi.org/10.1007/s10856-021-06591-x>.
96. Ahmed H.Y., Safwat N., Shehata R., Althubaiti E.H., Kareem S., Atef A., Qari S.H., Aljahani A.H., Al-Meshal A.S., Youssef M., Sami R. Synthesis of natural nano-hydroxyapatite from snail shells and its biological activity: antimicrobial, antibiofilm, and biocompatibility. *Membranes (Basel)* 2022; 12(4): 408, <https://doi.org/10.3390/membranes12040408>.
97. Granito R.N., Muniz Renno A.C., Yamamura H., de Almeida M.C., Menin Ruiz P.L., Ribeiro D.A. Hydroxyapatite from fish for bone tissue engineering: a promising approach. *Int J Mol Cell Med* 2018; 7(2): 80–90, <https://doi.org/10.22088/IJMCM.BUMS.7.2.80>.
98. Kodali D., Hembrick-Holloman V., Gunturu D.R., Samuel T., Jeelani S., Rangari V.K. Influence of fish scale-based hydroxyapatite on forcespun polycaprolactone fiber scaffolds. *ACS Omega* 2022; 7(10): 8323–8335, <https://doi.org/10.1021/acsomega.1c05593>.
99. Shaltout A.A., Allam M.A., Moharram M.A. FTIR spectroscopic, thermal and XRD characterization of hydroxyapatite from new natural sources. *Spectrochim Acta A Mol Biomol Spectrosc* 2011; 83(1): 56–60, <https://doi.org/10.1016/j.saa.2011.07.036>.
100. Pradeep S., Jain A.S., Dharmashekara C., Prasad S.K., Akshatha N., Pruthvish R., Amachawadi R.G., Srinivasa C., Syed A., Elgorban A.M., Al Kheraif A.A., Ortega-Castro J., Frau J., Flores-Holguín N., Shivamallu C., Kollur S.P., Glossman-Mitnik D. Synthesis, computational pharmacokinetics report, conceptual DFT-based calculations and anti-acetylcholinesterase activity of hydroxyapatite nanoparticles derived from acorus calamus plant extract. *Frontiers in Chemistry* 2021; 9, <https://doi.org/10.3389/fchem.2021.741037>.
101. Ghate P., Prabhu S.D., Murugesan G., Goveas L.C., Varadavenkatesan T., Vinayagam R., Lan Chi N.T.,

- Pugazhendhi A., Selvaraj R. Synthesis of hydroxyapatite nanoparticles using *Acacia falcata* leaf extract and study of their anti-cancerous activity against cancerous mammalian cell lines. *Environ Res* 2022; 214(Pt 2): 113917, <https://doi.org/10.1016/j.envres.2022.113917>.
- 102.** Susanto H., Taufiq A., Sunaryono, Imam Mawardi A., Hariyanto Y.A., Nicholas Gerry A., Tri Yunisa D., Rufiandita F., Faris, Nizarghazi, Alifi G., Lita Neldya P., Sinta Dewi M. The characterization of green materials of *Moringa oleifera* leaf powder (MOLP) from Madura Island with different preparation methods. *IOP Conference Series: Earth and Environmental Science* 2019; 276(1): 012005, <https://doi.org/10.1088/1755-1315/276/1/012005>.
- 103.** Domene-López D., Delgado-Marín J.J., Martín-Gullón I., García-Quesada J.C., Montalbán M.G. Comparative study on properties of starch films obtained from potato, corn and wheat using 1-ethyl-3-methylimidazolium acetate as plasticizer. *Int J Biol Macromol* 2019; 135: 845–854, <https://doi.org/10.1016/j.ijbiomac.2019.06.004>.
- 104.** Khlestkin V.K., Rozanova I.V., Efimov V.M., Khlestkina E.K. Starch phosphorylation associated SNPs found by genome-wide association studies in the potato (*Solanum tuberosum* L.). *BMC Genet* 2019; 20(Suppl 1): 29, <https://doi.org/10.1186/s12863-019-0729-9>.
- 105.** Luo M., Li Z., Su M., Gadd G.M., Yin Z., Benton M.J., Pan Y., Zheng D., Zhao T., Li Z., Chen Y. Fungal-induced fossil biomineralization. *Curr Biol* 2023; 33(12): 2417–2424.e2, <https://doi.org/10.1016/j.cub.2023.04.067>.
- 106.** Alorku K., Manoj M., Yuan A. A plant-mediated synthesis of nanostructured hydroxyapatite for biomedical applications: a review. *RSC Adv* 2020; 10(67): 40923–40939, <https://doi.org/10.1039/d0ra08529d>.
- 107.** Shi D., Tong H., Lv M., Luo D., Wang P., Xu X., Han Z. Optimization of hydrothermal synthesis of hydroxyapatite from chicken eggshell waste for effective adsorption of aqueous Pb(II). *Environ Sci Pollut Res Int* 2021; 28(41): 58189–58205, <https://doi.org/10.1007/s11356-021-14772-y>.
- 108.** Barakat N.A.M., Khalil K.A., Sheikh F.A., Omran A.M., Gaihre B., Khil S.M., Kim H.Y. Physicochemical characterizations of hydroxyapatite extracted from bovine bones by three different methods: extraction of biologically desirable HAp. *Materials Science and Engineering: C* 2008; 28(8): 1381–1387, <https://doi.org/10.1016/j.msec.2008.03.003>.
- 109.** Boudreau S., Hrapovic S., Liu Y., Leung A.C.W., Lam E., Kerton F.M. Isolation of hydroxyapatite from Atlantic salmon processing waste using a protease and lipase mixture. *RSC Sustainability* 2023; 1(6): 1554–1564, <https://doi.org/10.1039/d3su00102d>.
- 110.** Mohd Pu'ad N.A.S., Koshy P., Abdullah H.Z., Idris M.I., Lee T.C. Syntheses of hydroxyapatite from natural sources. *Heliyon* 2019; 5(5): e01588, <https://doi.org/10.1016/j.heliyon.2019.e01588>.
- 111.** Forero-Sossa P.A., Salazar-Martínez J.D., Giraldo-Betancur A.L., Segura-Giraldo B., Restrepo-Parra E. Temperature effect in physicochemical and bioactive behavior of biogenic hydroxyapatite obtained from porcine bones. *Sci Rep* 2021; 11(1): 11069, <https://doi.org/10.1038/s41598-021-89776-2>.
- 112.** Horta M.K. dos S., Westin C., da Rocha D.N., Campos J.B. de, Souza R.F.M. de, Aguilar M.S., Moura F.J. Hydroxyapatite from biowaste for biomedical applications: obtainment, characterization and in vitro assays. *Materials Research* 2023; 26, <https://doi.org/10.1590/1980-5373-mr-2022-0466>.
- 113.** Joschek S., Nies B., Krotz R., Göferich A. Chemical and physicochemical characterization of porous hydroxyapatite ceramics made of natural bone. *Biomaterials* 2000; 21(16): 1645–1658, [https://doi.org/10.1016/s0142-9612\(00\)00036-3](https://doi.org/10.1016/s0142-9612(00)00036-3).
- 114.** Cao X., Zhu J., Zhang C., Xian J., Li M., Nath Varma S., Qin Z., Deng Q., Zhang X., Yang W., Liu C. Magnesium-rich calcium phosphate derived from tilapia bone has superior osteogenic potential. *J Funct Biomater* 2023; 14(7): 390, <https://doi.org/10.3390/jfb14070390>.
- 115.** Gani M.A., Budiati A.S., Lestari M.L.A.D., Rantam F.A., Ardianto C., Khotib J. Fabrication and characterization of submicron-scale bovine hydroxyapatite: a top-down approach for a natural biomaterial. *Materials (Basel)* 2022; 15(6): 2324, <https://doi.org/10.3390/ma15062324>.
- 116.** Lee M.C., Seonwoo H., Jang K.J., Pandey S., Lim J., Park S., Kim J.E., Choung Y.H., Garg P., Chung J.H. Development of novel gene carrier using modified nano hydroxyapatite derived from equine bone for osteogenic differentiation of dental pulp stem cells. *Bioact Mater* 2021; 6(9): 2742–2751, <https://doi.org/10.1016/j.bioactmat.2021.01.020>.
- 117.** Yamamura H., da Silva V.H.P., Ruiz P.L.M., Ussui V., Lazar D.R.R., Renno A.C.M., Ribeiro D.A. Physico-chemical characterization and biocompatibility of hydroxyapatite derived from fish waste. *J Mech Behav Biomed Mater* 2018; 80: 137–142, <https://doi.org/10.1016/j.jmbbm.2018.01.035>.
- 118.** Acharya P., Kupendra M., Fasim A., Anantharaju K.S., Kottam N., Murthy V.K., More S.S. Synthesis of nano hydroxyapatite from Hypophthalmichthys molitrix (silver carp) bone waste by two different methods: a comparative biophysical and in vitro evaluation on osteoblast MG63 cell lines. *Biotechnol Lett* 2022; 44(10): 1175–1188, <https://doi.org/10.1007/s10529-022-03292-5>.
- 119.** Mathirat A., Dalavi P.A., Prabhu A., Devi G.V.Y., Anil S., Senthilkumar K., Seong G.H., Sargod S.S., Bhat S.S., Venkatesan J. Remineralizing potential of natural nano-hydroxyapatite obtained from epinephelus chlorostigma in artificially induced early enamel lesion: an in vitro study. *Nanomaterials (Basel)* 2022; 12(22): 3993, <https://doi.org/10.3390/nano12223993>.
- 120.** Athinarayanan J., Periasamy V.S., Alshatwi A.A. Simultaneous fabrication of carbon nanodots and hydroxyapatite nanoparticles from fish scale for biomedical applications. *Mater Sci Eng C Mater Biol Appl* 2020; 117: 111313, <https://doi.org/10.1016/j.msec.2020.111313>.
- 121.** Baek J.W., Kim K.S., Park H., Kim B.S. Marine plankton exoskeleton-derived hydroxyapatite/polycaprolactone composite 3D scaffold for bone tissue engineering. *Biomater Sci* 2022; 10(24): 7055–7066, <https://doi.org/10.1039/d2bm00875k>.
- 122.** Palaveniene A., Tamburaci S., Kimna C., Glambaite K., Baniukaitiene O., Tihminlioglu F., Liesiene J.

Osteoconductive 3D porous composite scaffold from regenerated cellulose and cuttlebone-derived hydroxyapatite. *J Biomater Appl* 2019; 33(6): 876–890, <https://doi.org/10.1177/0885328218811040>.

123. Fatimah I., Hidayat H., Purwiandono G., Khoirunisa K., Zahra H.A., Audita R., Sagadevan S. Green synthesis of antibacterial nanocomposite of silver nanoparticle-doped hydroxyapatite utilizing Curcuma longa leaf extract and land snail (*Achatina fulica*) shell waste. *J Funct Biomater* 2022; 13(2): 84, <https://doi.org/10.3390/jfb13020084>.

124. Mebarki M., Coquelin L., Layrolle P., Battaglia S., Tossou M., Hernigou P., Rouard H., Chevallier N. Enhanced human bone marrow mesenchymal stromal cell adhesion on scaffolds promotes cell survival and bone formation. *Acta Biomater* 2017; 59: 94–107, <https://doi.org/10.1016/j.actbio.2017.06.018>.

125. Ferraz M.P. Bone grafts in dental medicine: an overview of autografts, allografts and synthetic materials. *Materials (Basel)* 2023; 16(11): 4117, <https://doi.org/10.3390/ma16114117>.

126. Gibson I.R., Bonfield W. Novel synthesis and characterization of an AB-type carbonate-substituted hydroxyapatite. *J Biomed Mater Res* 2002; 59(4): 697–708, <https://doi.org/10.1002/jbm.10044>.

127. Siddiqi S.A., Azhar U. Carbonate substituted hydroxyapatite. In: Khan A.S., Chaudhry A.A. (eds). *Handbook of ionic substituted hydroxyapatites*. Woodhead Publishing; 2020; p. 149–173, <https://doi.org/10.1016/b978-0-08-102834-6.00006-9>.

128. Ishikawa K., Miyamoto Y., Tsuchiya A., Hayashi K., Tsuru K., Ohe G. Physical and histological comparison of hydroxyapatite, carbonate apatite, and β -tricalcium phosphate bone substitutes. *Materials (Basel)* 2018; 11(10): 1993, <https://doi.org/10.3390/ma11101993>.

129. Everts V., Delaissé J.M., Korper W., Jansen D.C., Tigchelaar-Gutter W., Saftig P., Beertsen W. The bone lining cell: its role in cleaning Howship's lacunae and initiating bone formation. *J Bone Miner Res* 2002; 17(1): 77–90, <https://doi.org/10.1359/jbmr.2002.17.1.77>.

130. Carrodeguas R.G., De Aza S. α -tricalcium phosphate: synthesis, properties and biomedical applications. *Acta Biomater* 2011; 7(10): 3536–3546, <https://doi.org/10.1016/j.actbio.2011.06.019>.

131. Crespi R., Cappare P., Gherlone E. Magnesium-enriched hydroxyapatite compared to calcium sulfate in the healing of human extraction sockets: radiographic and histomorphometric evaluation at 3 months. *J Periodontol* 2009; 80(2): 210–218, <https://doi.org/10.1902/jop.2009.080400>.

132. Atilgan S., Yaman F., Yilmaz U., Görgün B., Ünlü G. An experimental comparison of the effects of calcium sulfate particles and β -tricalcium phosphate/hydroxyapatite granules on osteogenesis in internal bone cavities. *Biotechnology & Biotechnological Equipment* 2007; 21(2): 205–210, <https://doi.org/10.1080/13102818.2007.10817446>.

133. Chen F., Wang M., Wang J., Chen X., Li X., Xiao Y., Zhang X. Effects of hydroxyapatite surface nano/micro-structure on osteoclast formation and activity. *J Mater Chem B* 2019; 7(47): 7574–7587, <https://doi.org/10.1039/c9tb01204d>.

134. Matsumoto M.A., Caviquili G., Bigueti C.C.,

Holgado Lde A., Saraiva P.P., Rennó A.C., Kawakami R.Y. A novel bioactive vitrocement presents similar biological responses as autogenous bone grafts. *J Mater Sci Mater Med* 2012; 23(6): 1447–1456, <https://doi.org/10.1007/s10856-012-4612-8>.

135. Bellucci D., Anesi A., Salvatori R., Chiarini L., Cannillo V. A comparative in vivo evaluation of bioactive glasses and bioactive glass-based composites for bone tissue repair. *Mater Sci Eng C Mater Biol Appl* 2017; 79: 286–295, <https://doi.org/10.1016/j.msec.2017.05.062>.

136. Bellucci D., Braccini S., Chiellini F., Balasubramanian P., Boccaccini A.R., Cannillo V. Bioactive glasses and glass-ceramics versus hydroxyapatite: comparison of angiogenic potential and biological responsiveness. *J Biomed Mater Res A* 2019; 107(12): 2601–2609, <https://doi.org/10.1002/jbm.a.36766>.

137. Souza E.Q.M., Costa Klaus A.E., Espósito Santos B.F., Carvalho da Costa M., Ervolino E., Coelho de Lima D., Fernandes L.A. Evaluations of hydroxyapatite and bioactive glass in the repair of critical size bone defects in rat calvaria. *J Oral Biol Craniofac Res* 2020; 10(4): 422–429, <https://doi.org/10.1016/j.jobcr.2020.07.014>.

138. Hayman A.R. Tartrate-resistant acid phosphatase (TRAP) and the osteoclast/immune cell dichotomy. *Autoimmunity* 2008; 41(3): 218–223, <https://doi.org/10.1080/08916930701694667>.

139. de Melo Pereira D., Davison N., Habibović P. Human osteoclast formation and resorptive function on biomineralized collagen. *Bioact Mater* 2021; 8: 241–252, <https://doi.org/10.1016/j.bioactmat.2021.06.036>.

140. Tayton E., Purcell M., Aarvold A., Smith J.O., Briscoe A., Kanczler J.M., Shakesheff K.M., Howdle S.M., Dunlop D.G., Oreffo R.O. A comparison of polymer and polymer-hydroxyapatite composite tissue engineered scaffolds for use in bone regeneration. An in vitro and in vivo study. *J Biomed Mater Res A* 2014; 102(8): 2613–2624, <https://doi.org/10.1002/jbm.a.34926>.

141. Yang W., Both S.K., Zuo Y., Birgani Z.T., Habibovic P., Li Y., Jansen J.A., Yang F. Biological evaluation of porous aliphatic polyurethane/hydroxyapatite composite scaffolds for bone tissue engineering. *J Biomed Mater Res A* 2015; 103(7): 2251–2259, <https://doi.org/10.1002/jbm.a.35365>.

142. Deng X., Huang B., Hu R., Chen L., Tang Y., Lu C., Chen Z., Zhang W., Zhang X. 3D printing of robust and biocompatible poly(ethylene glycol)diacrylate/nano-hydroxyapatite composites via continuous liquid interface production. *J Mater Chem B* 2021; 9(5): 1315–1324, <https://doi.org/10.1039/d0tb02182b>.

143. Ielo I., Calabrese G., De Luca G., Conoci S. Recent advances in hydroxyapatite-based biocomposites for bone tissue regeneration in orthopedics. *Int J Mol Sci* 2022; 23(17): 9721, <https://doi.org/10.3390/ijms23179721>.

144. Nakamura M., Hiratai R., Hentunen T., Salonen J., Yamashita K. Hydroxyapatite with high carbonate substitutions promotes osteoclast resorption through osteocyte-like cells. *ACS Biomater Sci Eng* 2016; 2(2): 259–267, <https://doi.org/10.1021/acsbiomaterials.5b00509>.

145. Heinemann C., Heinemann S., Rößler S., Kruppke B., Wiesmann H.P., Hanke T. Organically modified hydroxyapatite (ormoHAP) nanospheres stimulate the

differentiation of osteoblast and osteoclast precursors: a co-culture study. *Biomed Mater* 2019; 14(3): 035015, <https://doi.org/10.1088/1748-605X/ab0fad>.

146. Costa-Rodrigues J., Silva A., Santos C., Almeida M.M., Costa M.E., Fernandes M.H. Complex effect of hydroxyapatite nanoparticles on the differentiation and functional activity of human pre-osteoclastic cells. *J Biomed Nanotechnol* 2014; 10(12): 3590–3600, <https://doi.org/10.1166/jbn.2014.1873>.

147. Sun J.S., Lin F.H., Hung T.Y., Tsuang Y.H., Chang W.H.S., Liu H.C. The influence of hydroxyapatite particles on osteoclast cell activities. *J Biomed Mater Res* 1999; 45(4): 311–321, [https://doi.org/10.1002/\(sici\)1097-4636\(19990615\)45:4<311::aid-jbm5>3.0.co;2-9](https://doi.org/10.1002/(sici)1097-4636(19990615)45:4<311::aid-jbm5>3.0.co;2-9).

148. Han Y., Li S., Cao X., Yuan L., Wang Y., Yin Y., Qiu T., Dai H., Wang X. Different inhibitory effect and mechanism of hydroxyapatite nanoparticles on normal cells and cancer cells in vitro and in vivo. *Sci Rep* 2014; 4: 7134, <https://doi.org/10.1038/srep07134>.

149. Chen Z., Deng J., Cao J., Wu H., Feng G., Zhang R., Ran B., Hu K., Cao H., Zhu X., Zhang X. Nano-hydroxyapatite-evoked immune response synchronized with controllable immune adjuvant release for strengthening melanoma-specific growth inhibition. *Acta Biomater* 2022; 145: 159–171, <https://doi.org/10.1016/j.actbio.2022.04.002>.

150. Narducci P., Nicolin V. Differentiation of activated monocytes into osteoclast-like cells on a hydroxyapatite substrate: an in vitro study. *Ann Anat* 2009; 191(4): 349–355, <https://doi.org/10.1016/j.aanat.2009.02.009>.

151. Veillat V., Spuul P., Daubon T., Egaña I., Kramer I., Génot E. Podosomes: multipurpose organelles? *Int J Biochem Cell Biol* 2015; 65: 52–60, <https://doi.org/10.1016/j.biocel.2015.05.020>.

152. Ding X., Takahata M., Akazawa T., Iwasaki N., Abe Y., Komatsu M., Murata M., Ito M., Abumi K., Minami A.

Improved bioabsorbability of synthetic hydroxyapatite through partial dissolution-precipitation of its surface. *J Mater Sci Mater Med* 2011; 22(5): 1247–1255, <https://doi.org/10.1007/s10856-011-4291-x>.

153. Mestres G., Espanol M., Xia W., Persson C., Ginebra M.P., Ott M.K. Inflammatory response to nano- and microstructured hydroxyapatite. *PLoS One* 2015; 10(3): e0120381, <https://doi.org/10.1371/journal.pone.0120381>.

154. Ghanaati S., Udeabor S.E., Barbeck M., Willershausen I., Kuenzel O., Sader R.A., Kirkpatrick C.J. Implantation of silicon dioxide-based nanocrystalline hydroxyapatite and pure phase beta-tricalciumphosphate bone substitute granules in caprine muscle tissue does not induce new bone formation. *Head Face Med* 2013; 9: 1, <https://doi.org/10.1186/1746-160X-9-1>.

155. Li C., Yang L., Ren X., Lin M., Jiang X., Shen D., Xu T., Ren J., Huang L., Qing W., Zheng J., Mu Y. Groove structure of porous hydroxyapatite scaffolds (HAS) modulates immune environment via regulating macrophages and subsequently enhances osteogenesis. *J Biol Inorg Chem* 2019; 24(5): 733–745, <https://doi.org/10.1007/s00775-019-01687-w>.

156. Zeng Q., Wang R., Hua Y., Wu H., Chen X., Xiao Y.C., Ao Q., Zhu X., Zhang X. Hydroxyapatite nanoparticles drive the potency of Toll-like receptor 9 agonist for amplified innate and adaptive immune response. *Nano Res* 2022; 15(10): 9286–9297, <https://doi.org/10.1007/s12274-022-4683-x>.

157. Zhang L., Liang Z., Chen C., Yang X., Fu D., Bao H., Li M., Shi S., Yu G., Zhang Y., Zhang C., Zhang W., Xue C., Sun B. Engineered hydroxyapatite nanoadjuvants with controlled shape and aspect ratios reveal their immunomodulatory potentials. *ACS Appl Mater Interfaces* 2021; 13(50): 59662–59672, <https://doi.org/10.1021/acscami.1c17804>.